

# Instability of the interface between two inviscid fluids inside a rotating annulus in the absence of gravity

L. A. Dávalos-Orozco and E. Vázquez-Luis

*Instituto de Investigaciones en Materiales, Universidad Nacional Autónoma de México, Ciudad Universitaria, Apartado Postal 70-360, Delegación Coyoacán, 04510 México D.F., Mexico*

(Received 25 October 2002; accepted 12 June 2003; published 5 August 2003)

In this paper we investigate the linear instability of two superposed inviscid fluids between two rotating concentric cylinders. In the hydrostatic state the two fluids rotate as a rigid body with the same angular velocity as the annulus. Two problems are investigated. First, calculations are made of the instability of the liquid layer coating the outside of a cylinder under rotation. Second, results are obtained of the instability of two stratified fluids between two concentric cylinders. The first case is the most unstable condition of the second case when the outer fluid is absent. Therefore, in the second case only the instability of a system with a heavier fluid located outside the interface was investigated. It was found that the introduction of the inner cylinder produces new and interesting results about the axial and azimuthal modes not previously published in the literature. In particular, when a liquid layer coats the outside of a cylinder it was found that the azimuthal mode,  $n = 1$ , is the most important in a range of the nondimensional surface tension where the purely axial mode dominated in the absence of the inner cylinder. Additionally, it was found that some azimuthal spiral modes with a finite wavenumber appear as the most unstable in the presence of the inner cylinder. It was shown that the larger the centrifugal force is, the larger the nondimensional radius of the inner cylinder should be to make the instability more sensitive to the presence of the inner cylinder. An equation for the growth rate was obtained in the limit of very thin liquid layers and it was found that the maxima of growth rate agree very well with the experimental results of a fluid layer coating the outside of a rotating cylinder. © 2003 American Institute of Physics. [DOI: 10.1063/1.1597682]

## I. INTRODUCTION

In this paper the instability of two superposed inviscid fluids rotating at the same angular velocity (rigid body rotation) between two concentric cylinders in the absence of gravity was investigated (see Fig. 1). Due to the centrifugal force this system is hydrostatically stable if the heavier fluid is in contact with the external cylinder and it is unstable if that fluid is in contact with the inner cylinder.

The stability of this stratified system has important consequences in the coating of cylindrical surfaces when, for example, a liquid layer is applied to the external surface of a cylinder and the inertia and pressure of the outer gas is taken into account. The same applies with respect to the coating of the interior of a cylindrical surface.

The inner fluid is subjected to instabilities which were investigated more than a century ago by Rayleigh and reviewed by Chandrasekhar,<sup>1</sup> in the case of jets. One important characteristic of the axisymmetrical perturbations is that, to produce a throttling effect, their axial wavelengths need to be larger than the circumference of the cylindrical liquid column. Thus, under appropriate conditions, due to the radial surface tension this effect produces an instability such that the liquid cylinder starts to pinch at the troughs of the surface deformation until a drop is produced. When an inner cylinder is present, the throttling effect produces dry patches on its surface. These are, of course, very nonlinear effects.

Rayleigh<sup>2</sup> was interested in this phenomenon and he ob-

tained as a necessary and sufficient condition for instability that the circulation should decrease with the radius. The effect of surface tension and rotation was taken into account by Hocking and Michael.<sup>3</sup> They developed an analytical expression for the growth rate of longwave azimuthal perturbations (with zero axial wavenumber) of a liquid column under rotation. The instability was shown to appear when the magnitude of the surface tension force was small in comparison with the centrifugal force. The magnitude also depends on the azimuthal mode number considered.

In his paper Yih<sup>4</sup> focused on the instability of a thin liquid layer on a horizontal rotating cylinder. Yih showed that the critical wavenumber depends mainly on the surface tension and that the dependence on the Reynolds number [based on the fluid layer thickness ( $1.08 \times 10^{-3}$ – $8.17 \times 10^{-3}$  ft) and the angular velocity (9.01–29.4 rad)] was rather small. He showed experimentally that the perturbations are mainly axisymmetric using glycerine, a glycerine and water mixture and water alone.

Hocking<sup>5</sup> investigated the instability of a rigidly rotating liquid column under axisymmetric and longwave azimuthal perturbations. He found that the viscosity does not alter the stability criterion. In the case of longwave azimuthal perturbations the surface tension must be larger by a factor of 2 in order to stabilize the viscous liquid column.

Pedley,<sup>6</sup> in his paper, presented results on the swirling flow instability of a fluid with cylindrical free surface in the inside or on the outside. He found a necessary and sufficient

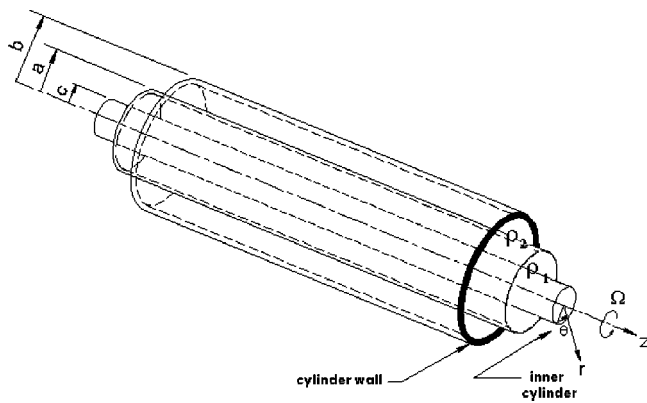


FIG. 1. Two fluid layers inside an annulus. All the system rotates as solid body. Here are shown the radius of the inner cylinder  $r=c$ , the interface  $r=a$  and the external cylinder  $r=b$ , respectively.

condition for the stability of the axisymmetric disturbances which requires, at the same time, satisfaction of Rayleigh's criterion of increasing circulation. Pedley was able to extend that condition to azimuthal perturbations for particular cases of swirling flows.

Joseph *et al.*<sup>7</sup> made calculations on the stability of stratified viscous liquids inside rotating cylindrical containers. They found, using the method of energy for nonlinear perturbations, that when the heavy fluid is outside the interface its radius remains constant depending on the positive magnitude of a nondimensional parameter which represents the ratio of the centrifugal and surface tension forces. When that parameter is negative the heavy fluid is inside and the interface destabilizes. They compared their results with experiments and their results agree with those of Moffatt<sup>8</sup> who also made experiments and used the lubrication approximation to obtain an equation for one liquid film coating the inside or the outside of a rotating cylinder.

Boudourides and Davis<sup>9</sup> extended the Rayleigh and Synge stability criteria for inviscid and viscous fluids to include a free surface. They looked for a sufficient condition for centrifugal, capillary and Rayleigh–Taylor stability.

Weidman<sup>10</sup> calculated the stability criteria for a system of two stratified fluids rotating rigidly inside a cylinder. His results generalized previous results where only one liquid layer was taken into account. Beside axisymmetric modes, azimuthal modes were considered for zero (longwave mode) and finite wavenumbers (spiral modes).

Weidman *et al.*<sup>11</sup> made a complete numerical analysis of the linear problem of two stratified inviscid fluids in rigid rotation inside a cylinder. They found the maxima of growth rate of instability for axisymmetric and azimuthal perturbations. However, they showed that for a rotating liquid column (which is the more unstable situation where the density of the outer fluid is negligible) only longwave azimuthal perturbations are the most unstable.

Concerning the papers on experiments related with the present problem those by Yih<sup>4</sup> and Moffatt<sup>8</sup> have already been mentioned. In them the instability of a liquid film coating the outside of a rotating cylinder was investigated. However, Moffatt<sup>8</sup> took into account the effect of gravity to un-

derstand the so called rimming flow. Additionally, experimental research has been performed by Joseph and his group,<sup>12–15</sup> on stratified fluids under rotation. However, their experiments were made for an inner very viscous fluid layer coating a cylinder rotating inside an initially static less viscous fluid. In other words, their results do not correspond to a rigid body rotation of all the system as supposed in the present paper, except for the rimming flows in air; however here the effect of gravity is important. They found interesting results related with rollers, coating and rimming flows.

Investigation of the instability of thin viscous liquid films flowing down vertical cylinders under rotation,<sup>16–18</sup> has shown that for certain values of the parameters the first azimuthal mode may be the most unstable. In the absence of rotation, but in the presence of thermocapillary effects, it has been shown that azimuthal modes up to 16 and over can be excited as the most unstable for some values of the parameters involved in the problem.<sup>19</sup>

These interesting results are the motivation to search for new results with respect to azimuthal modes in a system of stratified inviscid fluids similar to that studied by Weidman *et al.*<sup>11</sup> but including a new cylindrical solid boundary in the interior of the stratified fluids; that is, by the introduction of an inner concentric cylinder. As shown in Fig. 1, the system under investigation is composed of an annulus containing two stratified fluids with the characteristic that all is rotating as a solid body. The understanding of the behavior of the perturbations to this hydrostatic state is the subject of our research. When the radius of the inner cylinder tends to zero the system becomes that investigated by Weidman *et al.*<sup>11</sup>

The structure of the paper is as follows. In Sec. II, a description is given of the system under investigation, that is, two stratified inviscid liquids rotating rigidly between two concentric cylinders. Here, the equations of motion are introduced and, after subtracting the hydrostatic solution, the equations satisfied by the linear perturbations are obtained along with the corresponding boundary conditions. Section III is a review of important stability results relevant to our problem. Section IV presents results for the case of a liquid film coating a rotating cylinder. This is the most unstable situation of the two-layer system under investigation in which the heavier fluid is inside and the inertia of the outer fluid is so small that it can be neglected. It is divided into two subsections corresponding to the instability of axisymmetric and spiral perturbations, respectively. In Sec. V calculations are presented for the two-layer system when the heavier fluid is outside of the interface, and Sec. VI gives the conclusions. Finally, in order to complete the analytical calculations, an appendix is given at the end of the paper.

## II. EQUATIONS OF MOTION

The instability of two-superposed inviscid fluids rotating as a solid body between two concentric cylinders is investigated, and the effect of gravity has been neglected. A sketch of the system is shown in Fig. 1. In comparison with the paper of Weidman *et al.*<sup>11</sup> the inner cylinder with radius  $r=c$  is the new boundary condition, which as will be shown, brings about results not found previously in the literature.

The radius of the interface between the two fluids is at  $r = a$  and that corresponding to the external cylinder is at  $r = b$ . The fluids have constant densities  $\rho_i$  where  $i = 1$  and  $2$  for the inner and outer fluid, respectively. The angular velocity of the system is  $\mathbf{\Omega} = \Omega \mathbf{e}_z$ , where  $\Omega$  is the magnitude of the angular velocity vector and  $\mathbf{e}_z$  is a unit vector in the axial direction, here taken as  $z$ . The other unit vectors in the radial and azimuthal directions are  $\mathbf{e}_r$ ,  $\mathbf{e}_\theta$ , respectively. The surface tension constant of the interface is  $\gamma$ .

The equations of motion in cylindrical coordinates of an inviscid fluid in a rotating system are

$$\frac{D\mathbf{u}_i}{Dt} + 2\mathbf{\Omega} \times \mathbf{u}_i = -\frac{1}{\rho_i} \nabla p_i + \nabla \left[ \frac{(\mathbf{\Omega} \times \mathbf{r})^2}{2} \right] \quad (1)$$

along with the incompressibility equation

$$\nabla \cdot \mathbf{u}_i = 0. \quad (2)$$

Here,  $\mathbf{r}$  is the radius vector and  $r$  its magnitude and the vector  $\mathbf{u}_i = (u_i, v_i, w_i)$  is the velocity. The variables are made nondimensional as follows, the time with  $\Omega^{-1}$ , the length with the interface radius  $a$ , the velocity with  $a\Omega$  and the pressure with  $\rho_2 \Omega^2 a^2$ , respectively. In this way, the equations of motion of both fluids may be written as

$$\frac{\partial u_i}{\partial t} + (\mathbf{u}_i \cdot \nabla) u_i - \frac{v_i^2}{r} - 2v_i = -\frac{1}{\lambda^{2-i}} \frac{\partial}{\partial r} \left[ p_i - \frac{\lambda^{2-i}}{2} r^2 \right], \quad (3)$$

$$\frac{\partial v_i}{\partial t} + (\mathbf{u}_i \cdot \nabla) v_i - \frac{u_i v_i}{r} + 2u_i = -\frac{1}{\lambda^{2-i}} \frac{1}{r} \frac{\partial p_i}{\partial \theta}, \quad (4)$$

$$\frac{\partial w_i}{\partial t} + (\mathbf{u}_i \cdot \nabla) w_i = -\frac{1}{\lambda^{2-i}} \frac{\partial p_i}{\partial z}, \quad (5)$$

$$\frac{1}{r} \frac{\partial}{\partial r} (r u_i) + \frac{1}{r} \frac{\partial v_i}{\partial \theta} + \frac{\partial w_i}{\partial z} = 0, \quad (6)$$

where  $\lambda = \rho_1 / \rho_2$  is the densities ratio and the nabla operator in cylindrical coordinates is

$$\nabla = \frac{\partial}{\partial r} \mathbf{e}_r + \frac{1}{r} \frac{\partial}{\partial \theta} \mathbf{e}_\theta + \frac{\partial}{\partial z} \mathbf{e}_z.$$

Now, the interface is located at  $r = 1$ , the external cylinder at  $r = \kappa = b/a$  and the surface of the inner cylinder is at  $r = \kappa_1 = c/a$ . The perturbations to the interface are located at  $r = 1 + \eta(\theta, z, t)$ . This is used to calculate the normal vector at the interface:

$$\mathbf{n} = \left( \mathbf{e}_r + \frac{1}{r} \frac{\partial \eta}{\partial \theta} \mathbf{e}_\theta + \frac{\partial \eta}{\partial z} \mathbf{e}_z \right) \left[ 1 + \frac{1}{r^2} \left( \frac{\partial \eta}{\partial \theta} \right)^2 + \left( \frac{\partial \eta}{\partial z} \right)^2 \right]^{-1/2}.$$

Thus, the boundary conditions are

$$p_1 = p_0 \quad \text{at } r = \kappa_1, \quad (7)$$

$$u_1 = 0 \quad \text{at } r = \kappa_1, \quad (8)$$

$$u_2 = 0 \quad \text{at } r = \kappa, \quad (9)$$

where  $p_0$  is a reference pressure at the surface of the inner cylinder. The continuity of the radial velocities at the interface must be satisfied along with the kinematic boundary condition. That is

$$u_i - \left( \frac{\partial \eta}{\partial t} + \frac{v_i}{r} \frac{\partial \eta}{\partial \theta} + w_i \frac{\partial \eta}{\partial z} \right) = 0 \quad \text{at } r = 1 + \eta. \quad (10)$$

The pressure discontinuity at the interface is due to the surface tension and this can be expressed by means of a balance equation for the normal stresses

$$p_2 - p_1 = L_2 \nabla \cdot \mathbf{n} \quad \text{at } r = 1 + \eta. \quad (11)$$

In the hydrostatic state the system rotates as a rigid body and the pressure through each fluid satisfies, respectively,

$$p_{01} = p_0 + \frac{1}{2} \lambda (r^2 - \kappa_1^2), \quad \kappa_1 \leq r \leq 1, \quad (12)$$

$$p_{02} = p_0 + \frac{1}{2} r^2 + \frac{\lambda - 1}{2} - \frac{1}{2} \lambda \kappa_1^2 - L_2, \quad 1 \leq r \leq \kappa, \quad (13)$$

where  $L_i = \gamma / \rho_i \Omega^2 a^3$  is defined as the ratio of the surface tension force and the centrifugal force of fluid  $i = 1$  or  $2$  evaluated at the interface. It may be defined as the inverse of the centrifugal Bond number.

Applying small perturbations  $\mathbf{u}'_i$ ,  $p'_i$ ,  $\eta'$  to the velocity, pressure and surface deformation, respectively, the equations and boundary conditions can be linearized. In this way, the hydrostatic state of the system is perturbed as

$$\begin{pmatrix} \mathbf{u}_i \\ p_i \\ r \end{pmatrix} = \begin{pmatrix} 0 \\ p_{0i} \\ 1 \end{pmatrix} + \begin{pmatrix} \mathbf{u}'_i \\ p'_i \\ \eta' \end{pmatrix}. \quad (14)$$

After substitution in Eqs. (3)–(6) and subtraction of the hydrostatic solution, linearization gives the equations satisfied by the perturbations in each fluid region as follows:

$$\frac{\partial u'_i}{\partial t} - 2v'_i = -\frac{1}{\lambda^{2-i}} \frac{\partial p'_i}{\partial r}, \quad (15)$$

$$\frac{\partial v'_i}{\partial t} + 2u'_i = -\frac{1}{\lambda^{2-i}} \frac{1}{r} \frac{\partial p'_i}{\partial \theta}, \quad (16)$$

$$\frac{\partial w'_i}{\partial t} = -\frac{1}{\lambda^{2-i}} \frac{\partial p'_i}{\partial z}, \quad (17)$$

$$\frac{1}{r} \frac{\partial}{\partial r} (r u'_i) + \frac{1}{r} \frac{\partial v'_i}{\partial \theta} + \frac{\partial w'_i}{\partial z} = 0. \quad (18)$$

The linear boundary conditions for the perturbations are

$$u'_1 = 0 \quad \text{at } r = \kappa_1, \quad (19)$$

$$u'_2 = 0 \quad \text{at } r = \kappa, \quad (20)$$

$$u'_1 = u'_2 = \frac{\partial \eta'}{\partial t} \quad \text{at } r = 1, \quad (21)$$

$$p'_2 - p'_1 = -(1 - \lambda) \eta' + L_2 \left( \eta' + \frac{\partial^2 \eta'}{\partial \theta^2} + \frac{\partial^2 \eta'}{\partial z^2} \right) \quad \text{at } r = 1. \quad (22)$$

From here on the perturbations are supposed to be separable in normal modes as  $(u'_i, v'_i, w'_i, p'_i, \eta') = (U_i(r), V_i(r), W_i(r), P_i(r), A) e^{i(kz + n\theta) + st}$ , where  $U_i(r)$ ,  $V_i(r)$ ,  $W_i(r)$ ,  $P_i(r)$  and  $A$  are the amplitudes of the three components of velocity, the pressure and the interface, re-

spectively. Furthermore,  $k$  is the axial wavenumber,  $n$  is the azimuthal number and  $s = \sigma + i\omega$  is a complex number whose real part is the growth rate and the imaginary part is the frequency of oscillation of the perturbation. Therefore, in the normal modes, Eqs. (15)–(18) become equations for the amplitudes

$$sU_i - 2V_i = -\frac{1}{\lambda^{2-i}} DP_i, \tag{23}$$

$$sV_i + 2U_i = -\frac{in}{r\lambda^{2-i}} P_i, \tag{24}$$

$$sW_i = -\frac{ik}{\lambda^{2-i}} P_i, \tag{25}$$

$$\frac{1}{r} D(rU_i) + \frac{in}{r} V_i + ikW_i = 0, \tag{26}$$

with corresponding boundary conditions

$$U_1 = 0 \quad \text{at } r = \kappa_1, \tag{27}$$

$$U_2 = 0 \quad \text{at } r = \kappa, \tag{28}$$

$$U_1 = U_2 = sA \quad \text{at } r = 1, \tag{29}$$

$$P_2 - P_1 = -\Psi A \quad \text{at } r = 1, \tag{30}$$

where  $D \equiv d/dr$  and

$$\Psi = (1 - \lambda) - L_2(1 - n^2 - k^2). \tag{31}$$

### III. SOME PRELIMINARY RESULTS

Before numerical calculations are performed, it is necessary to know some analytical results obtained directly from the equations of motion. These results are useful to understand the stability of the system in particular cases when one of the parameters is small and to check the numerical results.

The results obtained by Weidman *et al.* in Appendix A of their paper<sup>11</sup> are also valid here because it is not necessary to make explicit use of the new boundary conditions. From those calculations the following sufficient condition for stability is obtained:

$$(1 - n^2 - k^2)L_2 < (1 - \lambda). \tag{32}$$

This means that perturbations with wavenumbers satisfying  $k < k_0$ , are unstable, where

$$k_0 = \sqrt{(1 - n^2) - \frac{1 - \lambda}{L_2}} \tag{33}$$

is the limit point of stability. The inequality in Eq. (32) and  $k_0$  in Eq. (33) will be useful in the search of unstable wavenumbers in the numerical analysis. When  $0 \leq \lambda \leq 1$ , the inner fluid has a smaller density than the outer one and the longwave ( $k=0, n \neq 0$ ) and spiral ( $|n| \geq 1, k \neq 0$ ) azimuthal modes are stable (see Appendix A of Weidman *et al.*<sup>11</sup>). However, the axisymmetric mode ( $n=0$ ) is unstable only when  $L_2 < (1 - \lambda)$ . Similarly, it can be shown that the axisymmetric mode is stationary.

The case  $\lambda^{-1} = 0$  is also of interest, since it corresponds to a liquid layer coating the outside of a cylinder under ro-

tation with a free surface. This case was investigated by Hocking and Michael<sup>3</sup> in the absence of inner and outer cylinders. Generalizing their analytical results it is found that our layer coating the inner cylinder is stable for longwave azimuthal perturbations ( $k=0$ ) when mode  $n$  satisfies

$$L_1 > \frac{n - C}{n(n^2 - 1)} \quad (n \geq 2), \tag{34}$$

where  $L_1 = \gamma/\rho_1\Omega^2 a^3$  and  $C = (1 - \kappa_1^{2n})/(1 + \kappa_1^{2n})$ . Thus, the liquid layer is unstable when this inequality is not satisfied and the longwave modes  $n \geq 1$  have (see the Appendix) the following growth rate:

$$\sigma_n = \sqrt{C\{(n-1)[1 - L_1 n(n+1)] + 1 - C\}}, \quad (n \geq 1). \tag{35}$$

This result reduces to that of Hocking and Michael<sup>3</sup> in the limit  $\kappa_1 \rightarrow 0$ , that is, when  $C=1$ . Note that, in Eq. (35), Hocking and Michael<sup>3</sup> only accept modes  $n \geq 2$  as physically possible; this is because, in the absence of an inner cylinder, mode  $n=1$  corresponds to a simple displacement of an infinite liquid column (in fact nothing happens). For that reason, in Eq. (35),  $\sigma_n = 0$  when  $n=1$  if  $\kappa_1 \rightarrow 0$  and  $k=0$ . However, in our case  $n=1$  is physically possible because now the inner cylinder plays the role of a reference point and the fluid layer appears, under rotation, as an eccentric cylinder with respect to the inner one. Moreover, if  $n=1$  is substituted into Eq. (35) the resulting  $\sigma_1 = \sqrt{C(1-C)}$  is constant with respect to  $L_1$  (and has the same value as that obtained numerically and presented in Figs. 5 and 6 for different  $\kappa_1$ ). The expression for  $\sigma_1$  can only be zero if  $C=0$  (no fluid at all) or if  $C=1$  (cylindrical liquid column<sup>3</sup>). Thus, for any  $0 < C < 1$ , this result shows that the longwave mode  $n=1$  is always unstable.

Now, it is of interest to calculate the maxima of the growth rate for different parameters. In the absence of the inner cylinder Pedley<sup>6</sup> and Weidman *et al.*<sup>11</sup> gave analytical and numerical results. They concluded that the azimuthal longwave ( $k=0$ ) modes are more unstable than the spiral modes ( $k \neq 0$ ). However, it should be noted that the spiral modes have not been investigated when the liquid layer is coating an inner cylinder under rotation. This is one of the goals of the present paper and will be discussed presently.

### IV. FLUID LAYER COATING THE OUTSIDE OF A CYLINDER UNDER ROTATION

Before going into the subject matter of this section some comments about the methods used to obtain the numerical results of the proper values  $n$ ,  $k$ , and  $s$ , in both cases of one and two fluid layers, are in order. First, the equations of the amplitudes and their boundary conditions Eqs. (23)–(30) are solved analytically obtaining complex equations for the growth rate and frequency of oscillation where they appear implicitly. In order to solve numerically these equations use was made of the IMSL subroutine in Fortran of the Newton–Rapson method. In some cases, the Müller method, useful to obtain roots of implicit complex functions, was used. An algorithm, which worked along with the subroutines, was designed to select the maxima of growth rate.

Now, the case of one fluid layer with a free surface coating the outside of a rotating cylinder is investigated. Note that this is the most unstable situation of a two-fluid layer system where the density of the outer fluid is negligible and its pressure is supposed constant (atmosphere). Therefore, it is of interest because the highest growth rate of instability is attained among all the two-layer system situations. This case corresponds to  $\lambda^{-1} = 0$ .

The perturbations satisfy Eqs. (23)–(31) but now with  $i = 1$  and the variables are made nondimensional using  $\rho_1$ . The velocity components can be eliminated to obtain an equation for the pressure

$$D^2 P_1 + \frac{1}{r} D P_1 - \left[ \frac{n^2}{r^2} + \alpha^2 \right] P_1 = 0, \tag{36}$$

where  $\alpha^2 = k^2(s^2 + 4)/s^2$ . The solution of this equation must be such that the radial component of velocity satisfies the impenetrability condition at the surface of the cylinder. That is

$$U_1 = -\frac{1}{(s^2 + 4)} \left( s D P_1 + \frac{2in}{r} P_1 \right) = 0 \quad \text{at } r = \kappa_1. \tag{37}$$

The solution for the pressure is

$$P_1(r) = A_1 I_n(\alpha r) + B_1 K_n(\alpha r), \tag{38}$$

where  $I_n(z)$  and  $K_n(z)$  are first and second Bessel functions, whose argument  $z$  is, in general, complex. Substitution of Eq. (38) into the boundary conditions Eqs. (30), (29) and (37) leads to the proper value equation for  $s$  with fixed  $k$ ,  $n$  and  $\kappa_1$

$$\alpha \left[ \begin{array}{c} I_n'(\alpha) - \frac{I_n'(\alpha\kappa_1) + \frac{2in}{\kappa_1} I_n(\alpha\kappa_1)}{K_n'(\alpha\kappa_1) + \frac{2in}{\kappa_1} K_n(\alpha\kappa_1)} K_n'(\alpha) \\ I_n(\alpha) - \frac{I_n(\alpha\kappa_1) + \frac{2in}{\kappa_1} I_n(\alpha\kappa_1)}{K_n(\alpha\kappa_1) + \frac{2in}{\kappa_1} K_n(\alpha\kappa_1)} K_n(\alpha) \end{array} \right] = \frac{s^2 + 4}{1 + (1 - k^2 - n^2)L_1} - \frac{2in}{s}. \tag{39}$$

Here, the primes mean that the derivative with respect to the argument of the Bessel functions has been taken. In addition, note that use has been made of the fact that  $\lambda^{-1} \rightarrow 0$  and that, as a consequence,  $\Psi/\lambda = -[1 + L_1(1 - n^2 - k^2)]$ . Moreover, the pressure has been made nondimensional using  $\rho_1$  instead of  $\rho_2$ . Taking the limit  $\kappa_1 \rightarrow 0$ , the proper value Eq. (39) reduces to that presented by Weidman *et al.*<sup>11</sup> for a liquid column under rotation.

**A. Fluid layer coating the outside of a cylinder under rotation: Axisymmetric case**

When the perturbations are axisymmetric ( $n = 0$ ) it was shown<sup>11</sup> that they must be stationary ( $\omega = 0$ ), that is,  $s = \sigma$ . In this way, the proper value Eq. (39) reduces to

$$\alpha \left[ \frac{I_0'(\alpha) + \frac{I_1(\alpha\kappa_1)}{K_1(\alpha\kappa_1)} K_0'(\alpha)}{I_0(\alpha) + \frac{I_1(\alpha\kappa_1)}{K_1(\alpha\kappa_1)} K_0(\alpha)} \right] = \frac{s^2 + 4}{1 + (1 - k^2)L_1}, \tag{40}$$

where  $\alpha = k\sqrt{\sigma^2 + 4}/\sigma$ . In order to understand the behavior of the system at a small rotation frequency, the limit  $\Omega \rightarrow 0$  is taken after returning to the dimensional form of the proper value equation. In nondimensional variables this limit gives

$$\sigma^2 \approx k(1 - k^2) \frac{I_0'(k) + \frac{I_1(k\kappa_1)}{K_1(k\kappa_1)} K_0'(k)}{I_0(k) + \frac{I_1(k\kappa_1)}{K_1(k\kappa_1)} K_0(k)} L_1, \quad (L_1 \rightarrow \infty). \tag{41}$$

In the limit  $\kappa_1 \rightarrow 0$ , this equation reduces to that presented by Weidman *et al.*,<sup>11</sup> which corresponds to that obtained by Rayleigh.<sup>20</sup>

Note that when  $k = 1$  there is no influence of  $L_1$  in Eq. (40). Therefore, for that wavenumber the growth rate  $\sigma$  depends only on  $\kappa_1$  for any centrifugal force. Figure 2 shows some examples of curves of  $\sigma$  against  $k$  for different values of  $\kappa_1$  and  $L_1$ . There is no difference between the curves of  $\kappa_1 = 0$  (no inner cylinder) and 0.5 except when  $L_1 = 10$  and 100 where the dashed line corresponds to  $\kappa_1 = 0.5$ . All the curves cross at  $k = 1$  and the crossing point corresponding to  $\kappa_1 = 0$  and 0.5 is at  $\sigma = 0.43323$  and for  $\kappa_1 = 0.9$  it is at  $\sigma = 0.28721$ . As seen in the figure, the growth rate decreases with increasing  $\kappa_1$  for  $0 \leq \kappa_1 \leq 1$ . The physical reason for this is that an increase of  $\kappa_1$  means that, for a fixed free surface radius, the radius of the inner cylinder increases diminishing the volume of the fluid layer, a situation which makes the system more stable. It is interesting that  $k = 1$  neutralizes the surface tension and the situation is just the nondimensional critical wavenumber found by Rayleigh for  $n = 0$  in the absence of rotation [see Eq. (41) and comments below]. In the presence of rotation the liquid layer is still unstable at  $k = 1$  because of the Rayleigh–Taylor instability.

The maxima of the growth rate can be calculated taking the derivative with respect to  $k$  of Eq. (40) where  $\sigma$  appears implicitly. After making  $\partial\sigma/\partial k = 0$ , the resulting expression is

$$L_1 = \frac{(\sigma + 4)(\kappa_1 G_1 + G_2) - \alpha(\kappa_1 G_3 + G_4)}{\alpha(1 - k^2)(\kappa_1 G_3 + G_4) - 2kG_2}, \tag{42}$$

where

$$\begin{aligned} G_1 &= I_0(\alpha)K_0(\alpha\kappa_1) - K_0(\alpha)I_0(\alpha\kappa_1), \\ G_2 &= I_0'(\alpha)K_0'(\alpha\kappa_1) - K_0'(\alpha)I_0'(\alpha\kappa_1), \\ G_3 &= I_0'(\alpha)K_0(\alpha\kappa_1) - K_0'(\alpha)I_0(\alpha\kappa_1), \\ G_4 &= I_0(\alpha)K_0'(\alpha\kappa_1) - K_0(\alpha)I_0'(\alpha\kappa_1). \end{aligned}$$

This expression for  $L_1$  is used in Eq. (40) to obtain an equation for the maximum growth rate and corresponding wavenumber  $\sigma_m$  and  $k_m$ , respectively, as functions of  $\kappa_1$ . These values are again entered in Eq. (42) to obtain the corresponding value of  $L_1$ . This procedure was used to calcu-

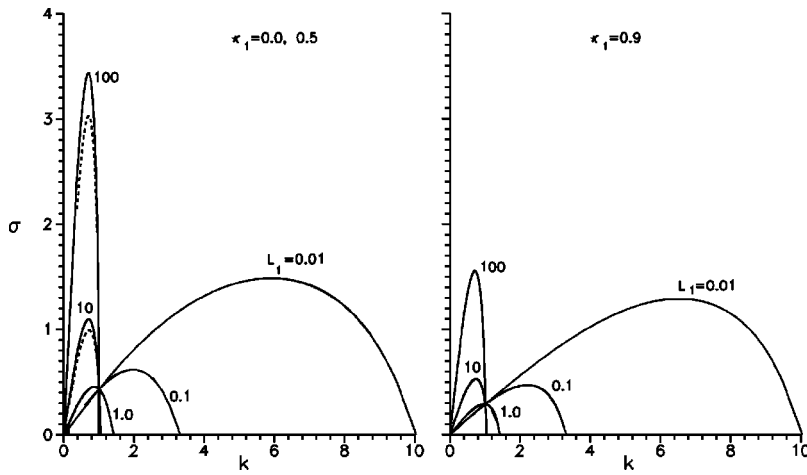


FIG. 2. Graphs of  $\sigma$  against  $k$  for different values of  $L_1$  and  $\lambda^{-1}=0$ . For  $\kappa_1=0$  and  $0.5$  (left figure) the curves superpose on each other except when  $L_1=10$  and  $100$  (dashed line is for  $\kappa_1=0.5$ ). The curves for  $\kappa_1=0.9$  are shown in the figure at the right hand side.

late the curves of the maximum growth rate against  $L_1$  of the axisymmetric mode given in Fig. 3. Note that the case  $\kappa_1=0$  is also included. The values of the maxima decrease with an increase of  $\kappa_1$ . The curves can be divided into two parts, one to the left of the minima where the rotation effects are important and another to the right where capillary effects are important. Note that all the curves tend to superimpose for large centrifugal forces.

Figure 4 shows the curves of the wavenumber corresponding to the maximum growth rate against  $L_1$ . Here, the general tendency is that the wavenumber decreases with  $L_1$ . The increase with  $\kappa_1$  is not very significant and it is observed only for small values of  $L_1$ .

It is of interest to compare our theoretical results with those observed by Yih<sup>4</sup> in his experiments. An important difference with the results presented above is that the fluid layers investigated by Yih are extremely thin. In order to obtain an analytical expression from our equations, an initial attempt was to make an expansion of Eq. (40) in terms of the small thickness of the layer. However, the result is not consistent because the coefficients of the terms of the expansion

depend on  $\alpha$  which was shown numerically to increase considerably when the layer thickness is very small. Therefore, because  $\alpha$  is part of the argument of the modified Bessel functions, it is necessary to take their asymptotic approximation for a very large argument. After some algebra, the following equation for the growth rate was obtained:  $k[1+(1-k^2)L_1]=\sigma\sqrt{\sigma^2+1}(1+2\kappa_1)/2\kappa_1$ . The differentiation with respect to  $k$  gives the wavenumber corresponding to the maximum growth rate. That is:  $k^2=(1+L_1)/3L_1$ . However, to put it in the nondimensional form used by Yih, it is necessary to make a change of parameters:  $L_1 \rightarrow S/b^3$  and  $k \rightarrow mb$ . Finally, in the notation used by Yih we have  $m^2=(1+S/b^3)b/3S$ , where  $1/b$  is the nondimensional liquid film thickness. If instead of  $S$  use is made of  $S_e$  (which includes the correction due to gravity in the upper side of the cylinder, where measurements were made) this equation agrees very well with the experimental results for the large (say  $Re > 40$ ) Reynolds numbers given in Table III of Ref. 4. Moreover, the wavenumbers of this equation agree perfectly

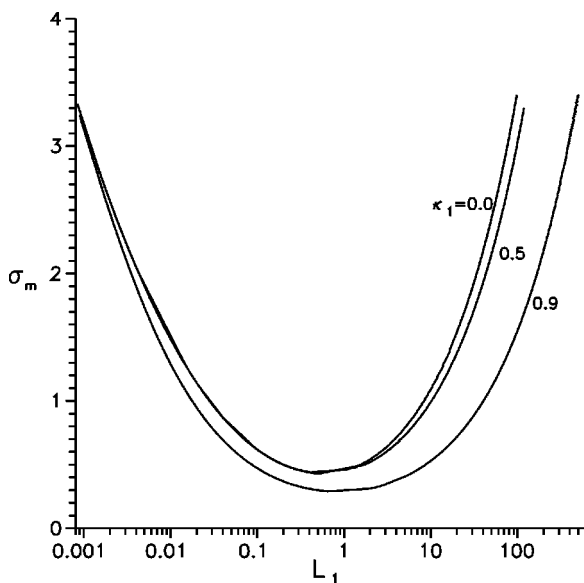


FIG. 3. The maximum growth rate against  $L_1$  for different values of  $\kappa$ .

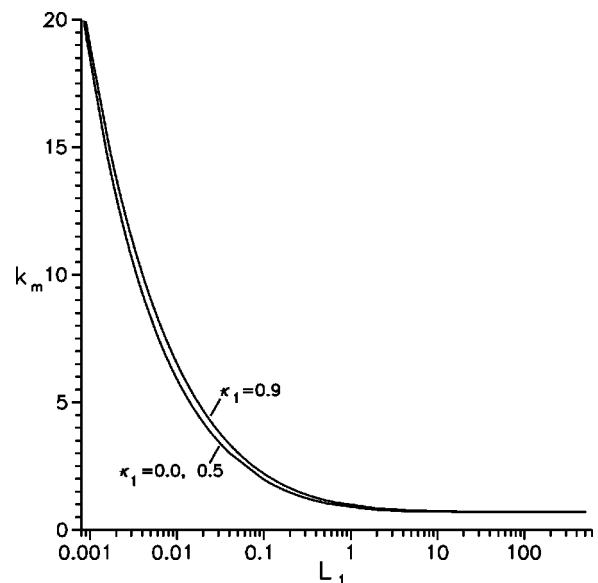


FIG. 4. The wavenumber corresponding to the maximum growth rate against  $\kappa_1$ .

well with the curves of  $m$  vs  $S$  given in Figs. 1 and 3 of the same reference.

### B. Fluid layer coating the outside of a cylinder under rotation: Spiral modes

As already shown,<sup>11</sup> the azimuthal spiral ( $n \geq 1, k \neq 0$ ) and longwave ( $n \geq 1, k = 0$ ) modes are time dependent and their frequency is  $\omega \neq 0$ ; therefore,  $s = \sigma + i\omega$  in Eq. (39). In this way, the exponential in the normal modes is expressed as  $\exp[i(kz + n\theta + \omega t) + \sigma t]$ . It is supposed that the rotation is right-handed (with the right hand thumb representing the rotation axis) or in the counter clockwise-direction. Therefore, a positive frequency of oscillation means that the azimuthal modes rotate in the clockwise direction when the  $n$  modes are positive. The stability of the mode  $n$  differs when it is positive or negative due to the action of the Coriolis force.<sup>17</sup>

The azimuthal longwave modes have an extremely large wavelength in the axial direction and therefore they look like the flutes in the columns used in the ancient Greek architecture but with an axial undulation at very large intervals. In this sense, the azimuthal spiral modes will also have axial deformation but at far shorter intervals (as in the classic coke bottle).

In order to obtain the maximum growth rate with more precision, it was necessary to calculate the curves of  $\sigma$  and  $\omega$  against  $k$  in a broad range of values of the parameters  $L_1$  and  $\kappa_1$ . This was done in order to be sure which mode is the most important, an azimuthal longwave or a spiral mode. In particular, for  $\kappa_1 = 0.5$  it was found that for the longwave azimuthal mode  $n=1$  the maximum growth rate is larger than that of  $n=0$  for the range of  $L_1$  between approximately  $0.22 < L_1 < 1.46$ . The minimum of the curve of  $n=0$  is found inside this range. This is an important difference with respect to the results obtained by Weidman *et al.*,<sup>11</sup> where the mode  $n=0$  is the dominant one. From values of  $L_1 = 1.46$  to  $L_1 \rightarrow \infty$  the axisymmetric mode is the most unstable. When  $L_1 < 0.22$  the axisymmetric mode again is the more unstable in a short range of values below which higher longwave modes are most unstable, as seen in Fig. 5. Decreasing  $L_1$  the mode  $n=2$  starts at  $L_1 = 0.1053$ . It should be noted that almost all the curves are the same as those of  $\kappa_1 = 0$  except when  $n = 1$ , as explained above, and when  $n=2$  which has a maximum growth rate somewhat higher.

Different results have been found for  $\kappa_1 = 0.9$  as shown in Fig. 6. The mode  $n=1$  is more unstable than mode  $n=0$  in the range  $0.18 < L_1 < 2.0$ , with the characteristic that  $n=0$  does not appear for a large centrifugal force. However, mode  $n=0$  is important for small centrifugal force when  $L_1 > 2.0$ .

Increasing the centrifugal force, that is decreasing  $L_1$ , transitions into higher modes appear sequentially. However, a new feature is that, for some mode numbers, the longwave modes appear first giving way, after some decrease of  $L_1$ , to a spiral mode ( $k \neq 0$ ) of the same azimuthal number. This is shown in Fig. 6 where the spiral mode section of the corresponding azimuthal number is represented by means of stars superposed on the curves. This result is new and happens when  $\kappa_1$  is a little less than and slightly larger than 0.9, that

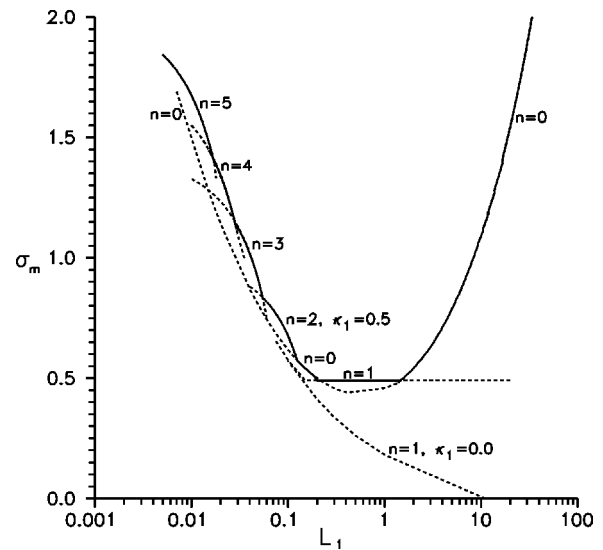


FIG. 5. The maximum growth rate against  $L_1$  for  $\kappa_1 = 0, 0.5$ . Longwave azimuthal modes. The continuous lines show the range of  $L_1$  where the corresponding mode is the most unstable.

is, when the liquid layer is thin. It occurs due to the presence of the inner cylinder when the liquid layer thickness is around 10% or less than the radius of the unperturbed free surface. It can be seen that, to the left of the minimum, the mode  $n=0$  no longer appears.

In Fig. 7 the same results are shown using a different scale for the  $L_1$  axis. In this way, it is clear that when spiral modes appear the curve is divided into two different parts. One is a continuous line corresponding to a longwave azimuthal mode and the other (starred) to the left corresponds to the spiral mode. As shown, only the spiral modes  $n=2, 3$  and  $4$  are able to appear for this value of  $\kappa_1$ . The spiral mode  $n=5$ , to the left of  $n=4$ , also exists but it is not the most unstable. In that range of  $L_1$  the most important longwave mode is that of  $n=6$ . The dashed lines indicate less unstable modes.

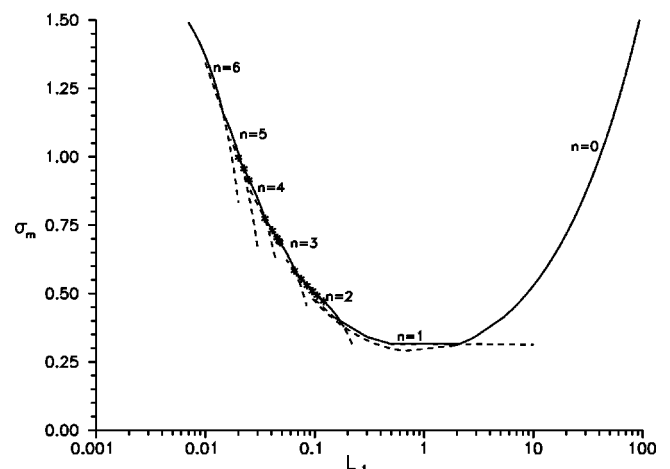


FIG. 6. The maximum growth rate against  $L_1$  for  $\kappa_1 = 0.9$ . Longwave and spiral azimuthal modes. The continuous lines show the  $L_1$  range where the longwave modes are the most unstable. The starred lines show the  $L_1$  range where the spiral modes are the most unstable.

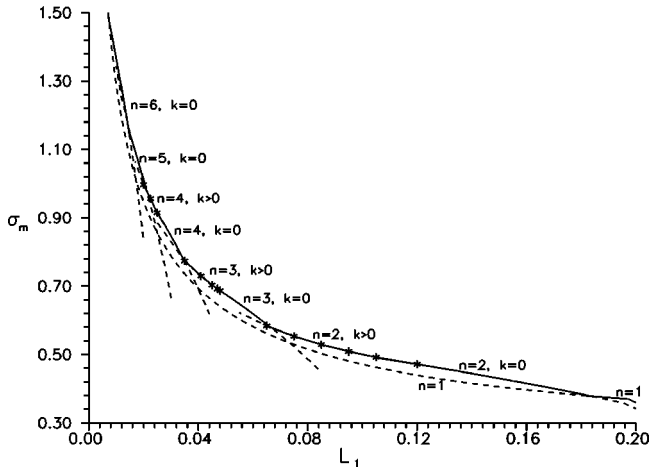


FIG. 7. An amplified view of Fig. 6 for  $\kappa_1 = 0.9$  showing the  $L_1$  range of spiral modes.

The mode  $n = 1$  was investigated in the range of  $\kappa_1$ . It was found that this mode is the most unstable for a wide part of the range. For example, Fig. 8 shows that for  $L_1 = 1$  the mode  $n = 0$  is the most unstable when  $\kappa_1 < 0.4$  and that mode  $n = 1$  is the most unstable for  $\kappa_1 > 0.4$ . The maximum growth rate of  $n = -1$  shows that this could never be the most unstable. It can be seen that the curve of the maximum growth rate for  $n = 1$  also has a maximum around  $\kappa_1 = 0.6$  after which the curve tends to zero.

## V. TWO STRATIFIED FLUIDS ROTATING BETWEEN TWO CONCENTRIC CYLINDERS

The proper value equation for the three dimensional perturbations of a two fluid system under rotation is more general and complex than that described in the earlier sections. In order to calculate this equation it is necessary to eliminate the velocity components, obtain equations for the pressure of each fluid and suppose the following solutions:

$$P_1(r) = A_1 I_n(\alpha r) + B_1 K_n(\alpha r), \quad (43)$$

$$P_2(r) = A_2 I_n(\alpha r) + B_2 K_n(\alpha r). \quad (44)$$

The boundary conditions for the pressures are obtained from those of the velocities. Therefore, conditions of Eqs. (27)–(30) can be translated into

$$sDP_1 + \frac{2in}{\kappa_1} P_1 = 0 \quad \text{at } r = \kappa_1, \quad (45)$$

$$sDP_2 + \frac{2in}{\kappa} P_2 = 0 \quad \text{at } r = \kappa, \quad (46)$$

$$(sDP_1 + 2inP_1) = \lambda(sDP_2 + 2inP_2) \quad \text{at } r = 1, \quad (47)$$

$$P_2 - P_1 = \frac{\Psi}{s^2 + 4} \left[ DP_2 + \frac{2in}{s} P_2 \right] \quad \text{at } r = 1. \quad (48)$$

Substitution of the solutions of Eqs. (43) and (44) into the boundary conditions leads to the more general proper value equation.

The situation of a fluid layer coating the outside of a rotating cylinder investigated in Sec. IV is the more unstable

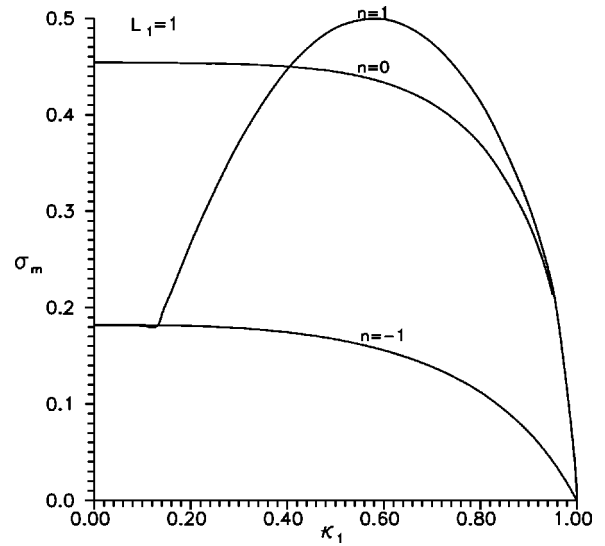


FIG. 8. The maximum growth rate against  $\kappa_1$  for  $L_1 = 1$  and  $n = -1, 0, 1$ .  $\sigma_m$  tends to zero when  $\kappa_1 \rightarrow 1$ . Note that  $\sigma_m$  also has a maximum.

case among the stratifications represented by the more general proper value equation. Therefore, here only the case where the outer fluid is more dense than the inner one will be investigated. Due to the centrifugal force this stratification is hydrostatically stable. However, the fluid is subjected to a throttling effect by the surface tension and to the Coriolis force which can cause destabilization under a variety of conditions. According to the results of Sec. III, the perturbations under this stratification are stable to both longwave and spiral azimuthal modes. Therefore, only axisymmetric perturbations will be investigated and these must be stationary.<sup>11</sup> In this way, taking  $n = 0$  and consequently  $s = \sigma$  the proper value equation is

$$\begin{aligned} & [\alpha \Psi_2 I_0'(\alpha) - \lambda(s^2 + 4)] F_1(\alpha, \beta) - (s^2 \\ & + 4) I_0'(\alpha) F_2(\alpha, \beta) + C' \{ [\alpha \Psi_2 I_0'(\alpha) - \lambda(s^2 \\ & + 4)] F_1(\alpha, \beta) - (s^2 + 4) I_0'(\alpha) F_2(\alpha, \beta) \} = 0, \end{aligned} \quad (49)$$

where

$$F_1(\alpha, \beta) = I_0'(\alpha) K_0'(\beta) - K_0'(\alpha) I_0'(\beta), \quad (50)$$

$$F_2(\alpha, \beta) = I_0(\alpha) K_0'(\beta) - K_0(\alpha) I_0'(\beta). \quad (51)$$

Here,  $C' = I_1(\alpha \kappa_1) / K_1(\alpha \kappa_1)$ ,  $\alpha = k \sqrt{\sigma^2 + 4} / \sigma$ ,  $\beta = \kappa \alpha$  and  $\Psi_2 = \Psi(n = 0) = 1 + L_2(k^2 - 1)$ . The growth rate can be obtained numerically for different values of  $\lambda$ ,  $L_2$ ,  $\kappa$  and  $\kappa_1$  inside the wavenumber range of the limit point of instability given by Eq. (33). Calculations were made for  $\lambda = 1/4$  and  $3/4$ ,  $\kappa_1 = 0.0, 0.5, \text{ and } 0.9$  and  $\kappa = 1.2$  and  $5$  in a wide range of  $L_2$  in order to find the correct maxima of growth rate. The curves of  $\sigma_m$  against  $L_2$  for  $\kappa = 1.2$  (the inner fluid with the inner cylinder occupying an 83% of the radial range of the system) are shown in Fig. 9. The growth rate is positive if  $L_2 > (1 - \lambda)$  and the limit points of instability intersect at the same point dependent on  $\lambda$  but independent of  $\kappa_1$ . As shown, the maximum growth rate depends on the radius of the inner cylinder and this dependence becomes important



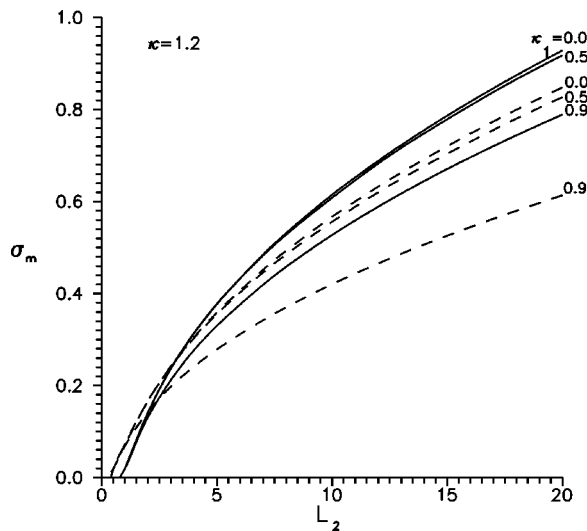


FIG. 9. Stably stratified fluids. The maximum growth rate against  $L_2$  for  $n=0$ ,  $\kappa=1.2$ ,  $\lambda=0.25$  (continuous line) and  $0.75$  (dashed line) and different values of  $\kappa_1$ . See Fig. 12 for the corresponding wavenumbers.

above  $\kappa_1=0.5$ , for thin liquid layers in the inside. The intersection point of the curves of  $\lambda=1/4$  and  $3/4$ , at some value of  $L_2$ , varies with  $\kappa_1$  (for  $\kappa_1=0$  it occurs around  $L_{2C} \approx 3.3$ ). This crossing point is important because it is counterintuitive that a condition which is more stable than another can become more unstable when the rotation is increased. The reason for the existence of this point is because the surface tension becomes less important than the centrifugal force as  $L_2$  decreases. When  $\rho_1 (<\rho_2)$  is near to  $\rho_2$  the inner fluid increases its possibility to penetrate the outer layer due to the effects of the centrifugal force on the perturbations. In this way, when the density of the inner fluid is smaller but near to that of the outer layer the system is more unstable for small  $L_2$  than when the inner fluid is far less denser. Additionally, it is clear that it is easier for surface tension to destabilize the system when the inner fluid is less dense than the outer one because its throttling effect, directed radially towards the interior, needs less force to remove the fluid with a lower inertia. The variation of  $L_2$  corresponding to the crossing points with respect to  $\kappa_1$  is shown in Fig. 10. Here, the results are for  $\kappa=1.2$  and  $5$ , and it can be seen that  $L_{2cr}$  decreases with  $\kappa_1$ . This means that a larger centrifugal force is needed to attain a crossing point when the inner liquid film becomes relatively thinner.

The maximum growth rate corresponding to the crossing point versus  $\kappa_1$  is shown in Fig. 11. When the inner liquid layer thickness tends to zero the growth rate also tends to zero, as expected, and the effect of  $\kappa_1$  is important only above  $0.6$ .

The variation of the wavenumber corresponding to the maximum growth rate (Fig. 9) against  $L_2$  is shown in Fig. 12. The curves overlap each other when  $\kappa_1$  is  $0$  and  $0.5$ . In the limiting case of  $L_2 \rightarrow \infty$  (zero rotation) the curves tend to the same value<sup>11</sup> independent of  $\lambda$  but still dependent on  $\kappa_1$ .

The maximum growth rate of the instability of a system with  $\kappa=5.0$  is shown in Fig. 13. Here, the inner fluid layer with the inner cylinder only fills 20% of the radial range. The

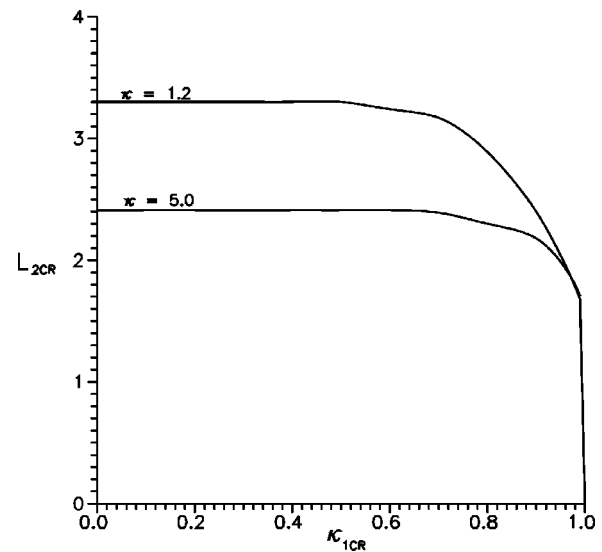


FIG. 10.  $L_{2cr}$  against  $\kappa_{1cr}$  for  $\kappa=1.2$  and  $5$ . Curves of the cross points of the graphs of  $\sigma_m$  against  $L_2$  corresponding to  $\lambda=0.25$  and  $0.75$ . Some cross points for particular values of  $\kappa_1$  are shown in Figs. 9 and 13.

presence of the inner cylinder produces a stronger effect, for the given parameters, as can be seen by the separation of the curves. The corresponding graphs of the crossing points are given in Figs. 10 and 11. From these it can be understood that the crossing points depend not only on  $\kappa_1$  but also on  $\kappa$ . Furthermore, in the limit  $\kappa_1 \rightarrow 0$  the value obtained by Weidman *et al.*<sup>11</sup> is reached.

The curves for the wavenumber corresponding to the maximum growth rate against  $L_2$  are given in Fig. 14 for  $\kappa=5$ . Here, the curves separate clearly after a certain magnitude of  $L_2$ , and in the limit of  $L_2 \rightarrow \infty$  it is found that  $k_m$  depends<sup>11</sup> both on  $\lambda$  and  $\kappa_1$ .

Another way to understand the effect of the inner cylinder is by means of curves of the maximum growth rate against  $\kappa_1$ . This is shown in Fig. 15 for a fixed value of  $\lambda$

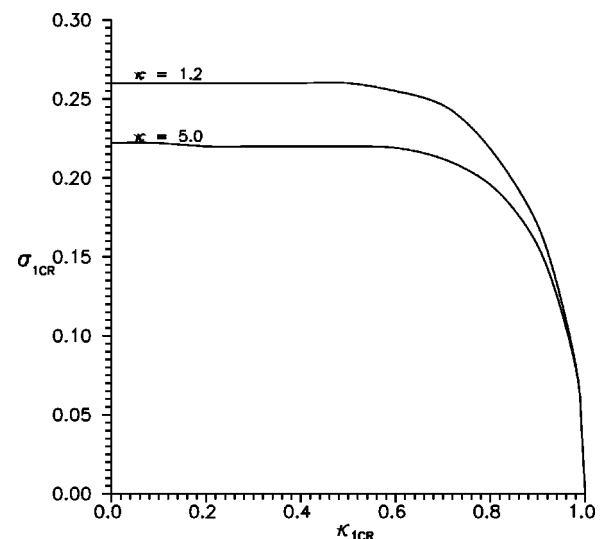


FIG. 11.  $\sigma_{mcr}$  against  $\kappa_{1cr}$  for  $\kappa=1.2$  and  $5$ . Curves of the cross points of the graphs of  $\sigma_m$  against  $L_2$  corresponding to  $\lambda=0.25$  and  $0.75$ . Some cross points for particular values of  $\kappa_1$  are shown in Figs. 9 and 13.

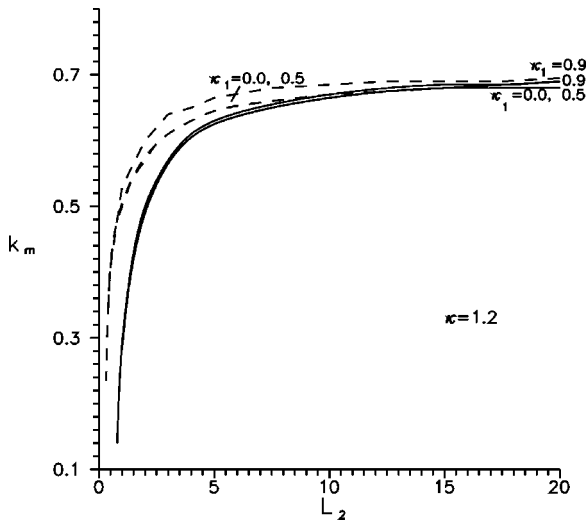


FIG. 12. The wavenumber corresponding to the maximum growth rate against  $L_2$  for  $\kappa=1.2$ ,  $\lambda=0.25$  (continuous line) and  $0.75$  (dashed line), and different values of  $\kappa_1$ .

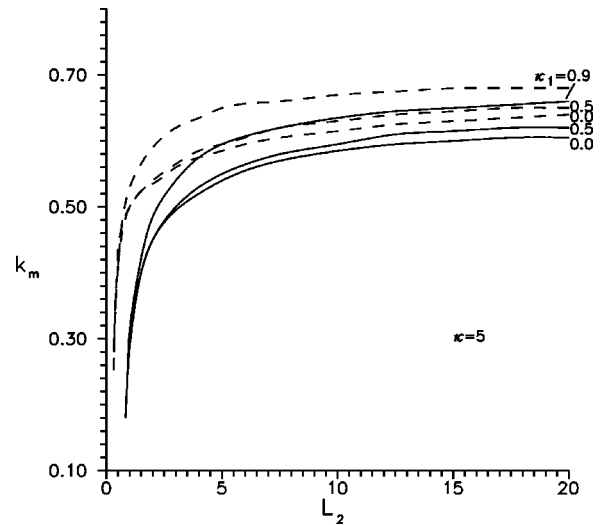


FIG. 14. The wavenumber corresponding to the maximum growth rate against  $L_2$  for  $\kappa=5$ ,  $\lambda=0.25$  (continuous line) and  $0.75$  (dashed line), and different values of  $\kappa_1$ .

$=0.25$  and two values of  $\kappa=1.2$  (dashed lines) and  $5$  (continuous lines). Only after some magnitude of  $\kappa_1$ , the value of  $\sigma_m$  has an important decrease towards zero. However, it should be noted that this effect is more important when  $\kappa=5$ . The smaller  $L_2$  is, the larger  $\kappa_1$  should be to make the system sensitive to the presence of the inner cylinder. When  $\kappa_1$  approaches 1 the growth rate tends to zero, as expected, because the inner fluid layer tends to disappear.

### VI. CONCLUSIONS

Our results make clear the importance of the influence of an inner cylinder on the instability of the system of two stratified fluids. When the inner liquid layer is coating the outside of the inner cylinder alone (no outside fluid) the problem represents the most unstable condition of a rotating

two-layer system: where the inner fluid has a larger density than the outer one. In this case, it has been shown that the azimuthal modes, longwave and spiral, play an important role on the instability. In particular, it has been shown that the  $L_1$  domain of the axisymmetric mode  $n=0$  is reduced due to the appearance of the azimuthal longwave mode  $n=1$  in the presence of the inner cylinder. This is an unexpected result because mode  $n=1$  does not appear when  $\kappa_1=0$ . The azimuthal spiral modes are the most important when the liquid layer is thin and the centrifugal force is large. However, these modes only appear in a fraction of the  $L_1$  range of the corresponding mode  $n \geq 2$ . An example was investigated for  $\kappa_1=0.9$  where the spiral modes are the most unstable when  $4 \geq n \geq 2$ . It was seen that the azimuthal spiral

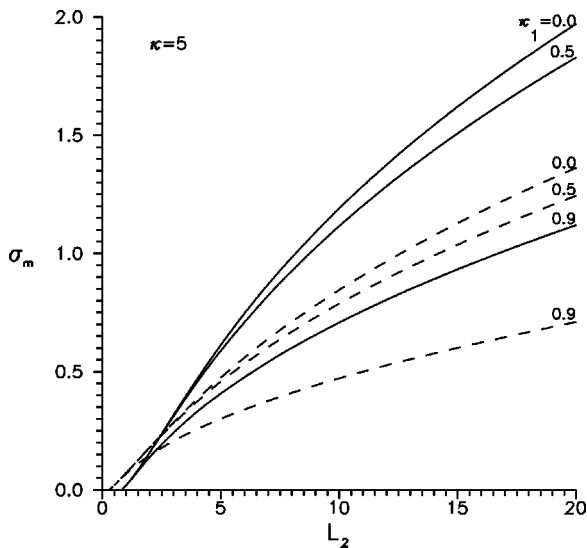


FIG. 13. The maximum growth rate against  $L_2$  for  $n=0$ ,  $\kappa=5$ ,  $\lambda=0.25$  (continuous line) and  $0.75$  (dashed line), and different values of  $\kappa_1$ . See Fig. 14 for the corresponding wavenumbers.

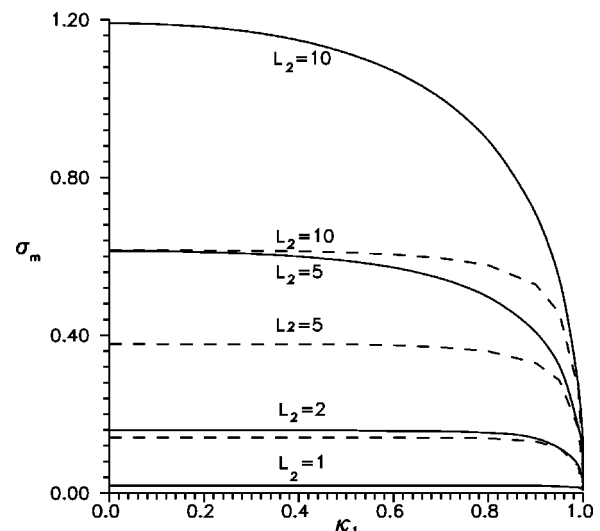


FIG. 15. The maximum growth rate against  $\kappa_1$  for  $\lambda=0.25$ ,  $\kappa=1.2$  (dashed line),  $\kappa=5$  (continuous line), and different values of  $L_2$ . The influence of  $\kappa_1$  on  $\sigma_m$  for  $\kappa=5$  is faster than for  $\kappa=1.2$ .

modes only appear as the most important in the presence of the inner cylinder, a result which is in contrast with the case of a rotating liquid column.

Additionally, by means of an asymptotic expansion of our equation in terms of  $\alpha$ , a formula for the wavenumber corresponding to the maximum growth rate of a perturbation in very thin fluid layers was found which agrees very well with the experimental results of Yih<sup>4</sup> when the magnitude of his rotation parameter is  $Re > 40$  and the correction of gravity is included. In this very thin fluid layer limit it was found that the azimuthal modes are not important.

When the stratification is reversed, that is, when the inner fluid is less dense than the outer one, the azimuthal modes are stable and consequently only the stationary axisymmetric mode was investigated. In order to understand the results obtained in this case let us suppose that the density of the outer fluid is fixed and that the density of the inner fluid can be varied. Under these conditions it was found that above a certain magnitude of  $L_2$  (the crossing point) the stratified system is more stable when the inner fluid increases its density. On the contrary, if  $L_2$  is below the crossing point an increase in density destabilizes the system. A physical explanation of these phenomena has been given in the paper and it was shown that the magnitude of the crossing point  $L_{2cr}$  depends on  $\kappa_1$  and  $\kappa$ . The dependence of the maximum growth rate on  $\kappa_1$  for various fixed magnitudes of  $L_2$  was also investigated and it was found that the larger the centrifugal force is, the larger  $\kappa_1$  should be in order for the system instability to be more sensitive to the presence of the inner cylinder. Moreover, it was found that the two-fluid layer instability is more sensitive to the inner cylinder when  $\kappa$  is large.

It is important to extend this investigation in the future to include in detail the viscous instability for the rotating system studied in this paper. The viscosity may be found to damp out some of the instability modes identified in this work, but it may be possible to find other instabilities arising due to the viscosity.

**ACKNOWLEDGMENTS**

The authors acknowledge support from DGAPA-UNAM to Project No. IN107502. E.V.L. would also like to thank support from CONACyT. L.A.D.O. would like to thank Cesar Díaz T., Caín González S. and Raúl Reyes O. for technical support. The authors would like to thank Professor Stephen Muhl for thoroughly reading the manuscript of the paper.

**APPENDIX: ANALYTIC CALCULATION OF THE GROWTH RATE OF LONGWAVE AZIMUTHAL PERTURBATIONS OF A LIQUID LAYER COATING THE OUTSIDE OF A CYLINDER UNDER ROTATION**

The goal of this appendix is to obtain an analytical expression for the growth rate of longwave azimuthal perturbations of the more general system investigated in this paper. The calculation starts following the method proposed by Hocking and Michael<sup>3</sup> for a rotating liquid column. The result is valid only for  $n \geq 1$ .

Under the assumption of irrotational flow the following potential  $\phi$  of the velocity perturbation is proposed in normal modes

$$\phi = f(r)e^{in\theta + st}. \tag{A1}$$

Here, the amplitude is supposed of the form

$$f(r) = A_1 r^n + A_2 r^{-n}, \tag{A2}$$

where  $n$  is a positive integer number. The free surface is located at  $r = 1$  and the surface of the inner cylinder is at  $r = \kappa_1$  in the nondimensional form. Thus, because the normal velocity is zero,  $f(r)$  satisfies

$$\frac{df}{dr} = 0 \quad \text{at } r = \kappa_1. \tag{A3}$$

In this way, the solution is

$$f(r) = A_1 k_1^n \left[ \left( \frac{r}{\kappa_1} \right)^n + \left( \frac{\kappa_1}{r} \right)^n \right]. \tag{A4}$$

A condition at the interface is the kinematic boundary condition

$$u - \frac{\partial \eta}{\partial \theta} = \frac{\partial \eta}{\partial t} \quad \text{at } r = 1 \tag{A5}$$

with a surface perturbation of the form

$$\eta = b e^{in\theta + st}, \tag{A6}$$

where  $b$  has the solution

$$b = -A_1 n \frac{1 - \kappa_1^{2n}}{s + in}. \tag{A7}$$

The pressure perturbation is obtained from the momentum equations, that is,

$$p = -iA_1 [2(1 - k_1^{2n}) + (s - n)(1 + k_1^{2n})] e^{in\theta + st}. \tag{A8}$$

The normal stress boundary condition is

$$p + \eta + L_1 \left( \eta + \frac{\partial^2 \eta}{\partial \theta^2} \right) = 0. \tag{A9}$$

Now, substitution of Eqs. (A7) and (A8) in (A9) leads to

$$[s + i(n - C)]^2 = C \{ (n - 1)[1 - L_1 n(n + 1)] + 1 - C \}, \tag{A10}$$

where  $C = (1 - k_1^{2n}/1 + k_1^{2n})$ . If the right-hand side of this equation is positive the real part of  $s$  is the growth rate. That is

$$\sigma_n = \sqrt{C \{ (n - 1)[1 - L_1 n(n + 1)] + 1 - C \}}, \quad (n \geq 1). \tag{A11}$$

When the axial wavenumber  $k$  tends to zero (longwave mode) this expression agrees with the growth rates calculated by means of numerical analysis of Eq. (39). These growth rates are maxima except when the spiral modes ( $k \neq 0$ ) and the axisymmetric mode are the most unstable.

<sup>1</sup>S. Chandrasekhar, *Hydrodynamic and Hydromagnetic Stability* (Dover, New York, 1981), Chap. 12.

<sup>2</sup>Lord Rayleigh, "On the dynamics of revolving fluids," Proc. London Math. Soc. **93**, 148 (1916).

- <sup>3</sup>L. M. Hocking and D. H. Michael, "The stability of a column of rotating liquid," *Mathematika* **6**, 25 (1959).
- <sup>4</sup>C.-S. Yih, "Instability of a rotating liquid film with a free surface," *Proc. R. Soc. London, Ser. A* **258**, 63 (1960).
- <sup>5</sup>L. M. Hocking, "The stability of rigidly rotating column of liquid," *Mathematika* **7**, 1 (1960).
- <sup>6</sup>T. J. Pedley, "The stability of rotating flows with a cylindrical free surface," *J. Fluid Mech.* **30**, 127 (1967).
- <sup>7</sup>D. D. Joseph, Y. Renardy, M. Renardy, and K. Nguyen, "Stability of rigid motions and rollers in bicomponent flows of immiscible liquids," *J. Fluid Mech.* **153**, 151 (1985).
- <sup>8</sup>H. K. Moffatt, "Behavior of a viscous film on the outer surface of a rotating cylinder," *J. Mec.* **16**, 651 (1977).
- <sup>9</sup>M. A. Boudourides and S. H. Davis, "Stability criteria for swirl flows with free surfaces," *Z. Angew. Math. Phys.* **37**, 597 (1986).
- <sup>10</sup>P. Weidman, "Stability criteria for two immiscible fluids rigidly rotating in zero gravity," *Rev. Roum. Sci. Tech., Ser. Mec. Appl.* **39**, 481 (1994).
- <sup>11</sup>P. D. Weidman, M. Goto and A. Fridberg, "On the instability of inviscid, rigidly rotating immiscible fluids in zero gravity," *Z. Angew. Math. Phys.* **48**, 921 (1997).
- <sup>12</sup>D. D. Joseph, K. Nguyen, and G. S. Beavers, "Non-uniqueness and stability of the configuration of flow of immiscible fluids with different viscosities," *J. Fluid Mech.* **141**, 319 (1984).
- <sup>13</sup>D. D. Joseph, Y. Renardy, M. Renardy, and K. Nguyen, "Stability of rigid motions and rollers in bicomponent flows of immiscible liquids," *J. Fluid Mech.* **153**, 151 (1985).
- <sup>14</sup>D. D. Joseph and L. Preziosi, "Stability of rigid motions and coating films in bicomponent flows of immiscible liquids," *J. Fluid Mech.* **185**, 323 (1987).
- <sup>15</sup>L. Preziosi and D. D. Joseph, "The run-off condition for coating and rimming flows," *J. Fluid Mech.* **187**, 99 (1988).
- <sup>16</sup>L. A. Dávalos-Orozco and G. Ruiz-Chavarría, "Hydrodynamic instability of a fluid layer flowing down a rotating cylinder," *Phys. Fluids A* **5**, 2390 (1993).
- <sup>17</sup>G. Ruiz-Chavarría and L. A. Dávalos-Orozco, "Stability of a liquid film flowing down a rotating cylinder subject to azimuthal disturbances," *J. Phys. II* **6**, 1219 (1996).
- <sup>18</sup>G. Ruiz-Chavarría and L. A. Dávalos-Orozco, "Azimuthal and streamwise disturbances in a fluid layer flowing down a rotating cylinder," *Phys. Fluids* **9**, 2899 (1997).
- <sup>19</sup>L. A. Dávalos-Orozco and X. You, "Three-dimensional instability of a liquid layer flowing down a heated vertical cylinder," *Phys. Fluids* **12**, 2198 (2000).
- <sup>20</sup>Lord Rayleigh, "On the instability of jets," *Proc. London Math. Soc.* **10**, 4 (1879).

Physics of Fluids is copyrighted by the American Institute of Physics (AIP).  
Redistribution of journal material is subject to the AIP online journal license and/or AIP  
copyright. For more information, see <http://ojps.aip.org/phf/phfcr.jsp>  
Copyright of Physics of Fluids is the property of American Institute of Physics and its  
content may not be copied or emailed to multiple sites or posted to a listserv without  
the copyright holder's express written permission. However, users may print,  
download, or email articles for individual use.